J Mol Model (2013) 19:4651–4659
DOI 10.1007/s00894-012-1428-x

ORIGINAL PAPER

Halogen bond tunability II: the varying roles of electrostatic and dispersion contributions to attraction in halogen bonds

Kevin E. Riley · Jane S. Murray · Jindřich Fanfrlík · Jan Řezáč · Ricardo J. Solá · Monica C. Concha · Felix M. Ramos · Peter Politzer

Received: 16 December 2011 / Accepted: 3 April 2012 / Published online: 29 May 2012

Abstract In a previous study we investigated the effects of aromatic fluorine substitution on the strengths of the halogen bonds in halobenzene…acetone complexes (halo= chloro, bromo, and iodo). In this work, we have examined the origins of these halogen bonds (excluding the iodo systems), more specifically, the relative contributions of electrostatic and dispersion forces in these interactions and how these contributions change when halogen σ-holes are modified. These studies have been carried out using density functional symmetry adapted perturbation theory (DFT-SAPT) and through analyses of intermolecular correlation energies and molecular electrostatic potentials. It is found that electrostatic and dispersion contributions to attraction in halogen bonds vary from complex to complex, but are generally quite similar in magnitude. Not surprisingly, increasing the size and positive nature of a halogen's σ-hole dramatically enhances the strength of the electrostatic component of the halogen bonding interaction. Not so obviously, halogens with larger, more positive σ-holes tend to exhibit weaker dispersion interactions, which is attributable to the lower local polarizabilities of the larger σ-holes.

Keywords Dispersion · Electrostatics · Halogen bonding · Noncovalent interactions

Electronic supplementary material The online version of this article (doi:10.1007/s00894-012-1428-x) contains supplementary material, which is available to authorized users.

K. E. Riley (✉) · J. Fanfrlík · J. Řezáč
Institute of Organic and Biochemistry, Academy of Sciences of the Czech Republic and Center for Biomolecules and Complex Molecular Systems,
166 10, Prague 6, Czech Republic
e-mail: kev.e.riley@gmail.com

R. J. Solá · F. M. Ramos
Department of Chemistry, University of Puerto Rico,
Rio Piedras Campus,
San Juan, Puerto Rico 00931

J. S. Murray · M. C. Concha · P. Politzer
CleveTheoComp,
1951 W. 26th Street,
Cleveland, OH 44113, USA

Introduction

Halogen bonding

Halogen bonding offers a rich array of possibilities for the design of new materials, in areas ranging from electronics to pharmaceuticals [1, 2]. There is also increasing recognition of its importance in biochemistry and molecular biology, for instance in the binding of ligands to proteins [3–6]. This diversity reflects the "tunability" of halogen bonding; it can be modified not only by changing the molecular environment of the halogen (e.g., making it more or less electron-withdrawing [7]) but also by changing the halogen itself. For instance, iodobenzene interacts more strongly with a Lewis base than does bromobenzene. However if the presence of iodine should be undesirable for a particular application, 3,5-difluorobromobenzene has been shown to interact equally well [8].

Halogen bonding is due to the presence of regions of positive electrostatic potential on the outer portions of many covalently-bonded halogens X, along the extensions of the bonds to the halogens; see Figs. 1 and 2 [4, 9, 10]. Through these positive regions, they can interact electrostatically with negative sites, such as the lone pairs of Lewis bases B. The resulting complexes, R-X...B, are typically characterized by

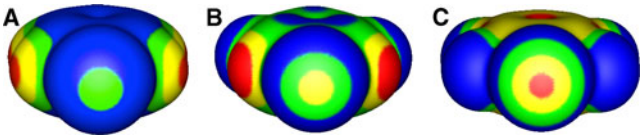

Fig. 1 Computed electrostatic potentials on 0.001 au molecular surfaces of chlorobenzene (**a**), 3,5-difluorochlorobenzene (**b**) and pentafluorochlorobenzene (**c**). The chlorine is facing the viewer in each case. Color ranges, in kcal mol^{-1}, are: red, greater than 20; yellow, between 20 and 10; green, between 10 and 0; blue, negative

the X…B separations being less than the sums of the respective van der Waals radii and the angles R-X…B being close to 180°, i.e., the interactions are essentially linear (barring secondary interactions that influence these angles [8, 11]).

The positive potentials on the halogens are the results of their anisotropic charge distributions, which show depletions of electronic density on the sides of the halogens opposite to the bonds R-X [12–16]. The regions of diminished electron density have been labeled "σ-holes" [17]. If the depletion is sufficient, the σ-hole acquires a positive electrostatic potential, i.e., a positive σ-hole, which can interact with a negative site. σ-holes are always along the extensions of the bonds to the halogens; this accounts for the directionality of halogen bonding. If the anisotropy of halogen X is not sufficient for its σ-hole to have a positive potential, then it will be negative, although less so than the surrounding region on the atom. It should be noted that the electrostatic interaction in halogen bonding always involves mutual polarization, of R-X by the electric field of B and of B by the electric field of the positive σ-hole on X [18].

For a given R, the σ-hole potential on the halogen X in R-X becomes more positive in the order F<< Cl<Br<I (following the trend in the halogens' polarizabilities) [4, 9, 10]. It is also more positive as R is more electron-withdrawing. For a given B, the binding energy of the complex R-X…B increases as the potential of the σ-hole of X becomes more positive [7, 8, 19].

The combination of electrostatics and polarization is a major directional driving force in halogen bonding [10]. Dispersion also plays an important role [7, 20]. These are partially balanced by a repulsive interaction, which becomes dominant at very short X…B separations. Our objective in this work has been to investigate and approximately quantify the relative contributions of electrostatics/polarization and dispersion, and how they depend upon the separation, the particular halogen and its molecular environment.

Interaction energies

It is sometimes conceptually useful to think of an interaction energy as composed of contributions from various factors – electrostatics, polarization, charge transfer, dispersion, orbital interaction, exchange repulsion, etc. – as is commonly done in perturbation theory techniques [21–23]. However it should be kept in mind that there is no rigorous basis for defining such contributions [22]. Only the overall interaction energy is a physical observable. A fundamental problem is that the proposed components are not independent of each other. For example, polarization is an intrinsic part of the electrostatic interaction. And where is the boundary between polarization and charge transfer [24, 25]? As Chen and Martínez pointed out [24], "…charge transfer is an extreme manifestation of polarization, …" It is accordingly not surprising that the various procedures that have been proposed for decomposing interaction energies sometimes lead to contradictory conclusions; for an example, see Politzer *et al.* [10].

Nevertheless, even taking note of these limitations, it is possible to estimate the electrostatic and the dispersion portions of noncovalent interaction energies. For the former, one can calculate the Coulombic interaction between the unperturbed ground-state charge distributions of the participants in the complex [21, 26]. This is a well-defined quantity, and while it neglects the accompanying polarization, it should give at least a lower bound to the magnitude of the actual electrostatic/polarization interaction energy. Earlier work suggests that polarization can usually be expected to augment this by less than about 25% [7, 26, 27].

The dispersion portion of the interaction energy is associated with the intermolecular electronic correlation [28–30]. Correlation energy is also well defined, as the difference between exact and true Hartree-Fock energies. Accordingly, we will take the difference between accurate

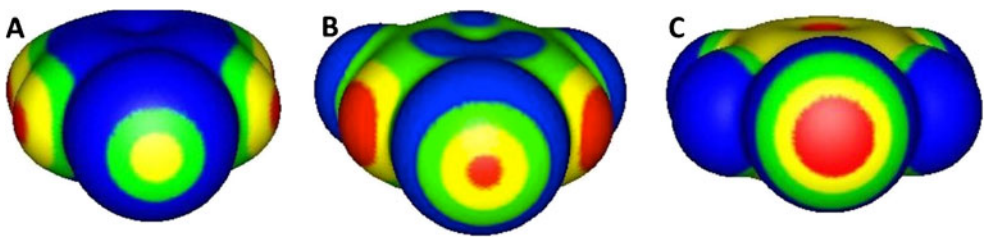

Fig. 2 Computed electrostatic potentials on 0.001 au molecular surfaces of bromobenzene (**a**), 3,5-difluorobromobenzene (**b**) and pentafluorobromobenzene (**c**). The bromine is facing the viewer in each case. Color ranges, in kcal mol^{-1}, are: red, greater than 20; yellow, between 20 and 10; green, between 10 and 0; blue, negative

correlated and Hartree-Fock interaction energies, labeled ΔE_{corr}, as an approximation to the dispersion energy [30]. While ΔE_{corr} reflects not only the intermolecular correlation but also the changes in intramolecular correlation of the halobenzene and acetone, these changes should be very small since we will maintain the ground-state geometries of these molecules. We will compare our ΔE_{corr} with the dispersion energies predicted by the widely-used symmetry-adapted perturbation theory (SAPT) [21, 23].

Methods

We have investigated six halobenzene-acetone complexes; the halobenzenes and their identifying labels are shown below in Scheme 1. The interactions are through the positive σ-holes on the halogens X, where X=Cl or Br. Acetone was chosen to be the Lewis base because (a) it has been shown to form strong halogen bonds [7] and (b) it is among the simplest models of the carbonyl groups found in biological systems.

Our procedure for optimizing the geometries of the complexes has been described in detail earlier [8]; it can be summarized as follows (see Fig. 3):

(1) The geometries of the free halobenzenes and acetone were optimized using gradient techniques at the density functional B3LYP/6-31+G(d) level, and were subsequently kept fixed.

The next three steps were carried out with the MP2/aug-cc-pVDZ procedure.

(2) Potential energy curves were generated for the complexes along the X…O separations, holding both the C-X…O and the X…O=C angles at 180°.
(3) At the X…O energy minima, the angles X…O=C were allowed to vary.
(4) Using the optimum X…O=C angles, potential energy curves along the X…O separations were again obtained. The resulting minimum energy structures were taken to be the final representations of the complexes.

The preceding optimization technique was employed in order to maintain the C-X…O angle at 180°. This ensured

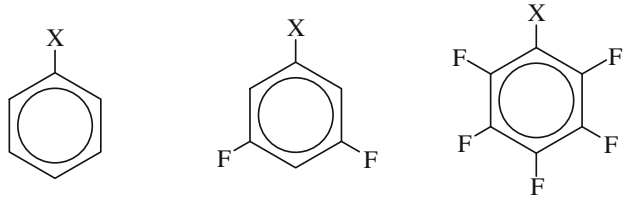

X-benz; X = Cl, Br X-benz-2F X-benz-5F

Scheme 1 Configurations of halogen bond donors considered in this work

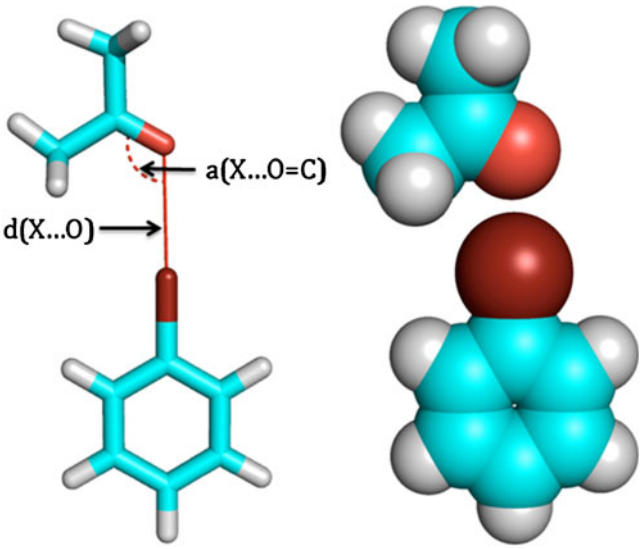

Fig. 3 Schematic models of halogen bonding in the complexes studied in this work

that the dominant interaction is the X…O halogen bond, with minimal contributions from secondary interactions such as are sometimes observed [8, 11, 31, 32].

The halobenzene and acetone geometries from step (1) above were also utilized to construct Hartree-Fock/aug-cc-pVDZ potential energy curves along the X…O separations. The optimized MP2 X…O=C angles were used.

The interaction energies as functions of the X…O separations, ΔE(X…O), were calculated with Eq. (1):

$$\Delta E(X\ldots O) = E_{complex}(X\ldots O) - [E_{halobenzene} + E_{acetone}]. \quad (1)$$

$E_{complex}(X\ldots O)$, $E_{halobenzene}$ and $E_{acetone}$ are the computed energies at 0 K of the complex at the separation X…O and the free halobenzene and acetone molecules. No zero-point energies are included. Counterpoise corrections were used to account for the basis set superposition error [33]. The dispersion contributions to the interaction energies at the various separations were approximated by $\Delta E_{corr}(X\ldots O)$, which is the difference between the corresponding MP2 and Hartree-Fock ΔE:

$$\Delta E_{corr}(X\ldots O) = \Delta E_{MP2}(X\ldots O) - \Delta E_{HF}(X\ldots O). \quad (2)$$

Potential energy curves and interaction energies were also computed by means of density functional symmetry-adapted perturbation theory (DFT-SAPT) [21, 23, 34, 35], with the LPBEOAC functional [36] and the aug-cc-pVTZ [37] basis set. In SAPT, the interaction energy is written as a sum of first- and second-order terms, which are commonly combined into electrostatic, induction, dispersion and exchange contributions. In DFT-SAPT a term accounting for higher order effects (mainly from induction), δHF, also contributes to the interaction energy [34, 35, 38]. The

electrostatic energy, E_{electr}, is determined as the Coulombic interaction between the unperturbed ground-state reactants. We will use E_{electr} as our measure of the electrostatic interaction and both ΔE_{corr} and the DFT-SAPT dispersion term, E_{disp}, to represent dispersion.

In view of the key role of the electrostatic potential in halogen bonding, we have calculated this for each of the six halobenzenes, focusing particularly upon the chlorine and bromine σ-holes. The electrostatic potential $V(\mathbf{r})$ that the nuclei and electrons of a molecule create at any point $\mathbf{r}$ is given by:

$$V(\mathbf{r}) = \sum_A \frac{Z_A}{|\mathbf{R}_A - \mathbf{r}|} - \int \frac{\rho(\mathbf{r}')d\mathbf{r}'}{|\mathbf{r}' - \mathbf{r}|}. \quad (3)$$

In Eq. (3), Z_A is the charge on nucleus A, located at $\mathbf{R}_A$, and $\rho(\mathbf{r})$ is the molecule's electronic density.

$V(\mathbf{r})$ is a physical observable, which can be determined experimentally by diffraction methods [39, 40] as well as computationally. Its sign in any region depends upon whether the positive contribution of the nuclei or the negative one of the electrons is dominant there.

The electrostatic potential is a quantity of fundamental importance [41]. Ayers has shown that knowledge of $V(\mathbf{r})$ suffices to completely characterize a molecular system [42], and atomic and molecular energies have been expressed as exact functionals of $V(\mathbf{r})$ [43]. It is an effective guide to the interpretation and prediction of noncovalent interactions [41, 44]; a variety of condensed phase properties that depend upon such interactions can be represented analytically in terms of statistically-defined features of $V(\mathbf{r})$.

In analyzing interactive behavior, we generally evaluate $V(\mathbf{r})$ on the molecular "surface" [45], since this is what is "seen" by an approaching entity. Following Bader *et al.* [46], we take the surface to be the 0.001 au (electrons/bohr^3) contour of the molecule's electronic density. This has the advantage of reflecting specific aspects of the molecule, such as lone pairs, π electrons, atomic anisotropies, etc. In this work, the electrostatic potentials were computed with the B3PW91/6-311G* procedure using the WFA-SAS code [45], to be consistent with earlier studies of fluorinated halobenzene molecules [8].

Results

Electrostatic potentials of halobenzenes

Figures 1 and 2 present the computed electrostatic potentials on the 0.001 au surfaces of the six halobenzenes being considered. The three with X=Cl are in Fig. 1, the X=Br are in Fig. 2. The chlorines and bromines are in the centers of the figures, and the positive σ-holes are clearly visible. These become larger and more positive as the number of electron-attracting fluorines on the ring increases and in going from X=Cl to X=Br. These trends are typical [4, 10], as was mentioned earlier. In Table 1 are listed the values of the most positive potentials, the $V_{S,max}$, that are associated with the σ-holes of the chlorines and bromines.

Note that each positive σ-hole is surrounded by negative electrostatic potential on the lateral sides of the chlorine or bromine. This accounts for the observed ability of many covalently-bound halogens to interact linearly through their σ-holes with nucleophiles (halogen bonding) and laterally with electrophiles [4, 7, 10, 47–50]. It also brings out the fallacy of assigning a single positive or negative charge to a covalently-bonded halogen.

Figures 1 and 2 show a marked similarity between the σ-hole potentials of the chlorine in Cl-benz-2F and the bromine in Br-benz; this is confirmed by their $V_{S,max}$, which are 11.9 and 12.2 kcal mol^{-1}, respectively (Table 1). Such a similarity is also seen in the chlorine σ-hole of Cl-benz-5F and the bromine σ-hole of Br-benz-2F; the $V_{S,max}$ are 18.9 and 18.4 kcal mol^{-1}. Since the magnitudes of the $V_{S,max}$ of σ-holes are a major determinant of the strengths of ensuing interactions [7, 8, 19], these examples show how halogen bonding can be "tuned" by appropriate choices of the halogen and substituents [8].

Properties of complexes with acetone

Table 1 also includes the MP2 optimum X…O separations, X…O=C angles and interaction energies ΔE of the six complexes with acetone. The X…O distances are all less than the sums of the relevant van der Waals radii, which are 3.28 Å for Cl…O and 3.37 Å for Br…O [51]. The X…O=C angles are in the neighborhood of 120°, which is consistent with the σ-hole interacting with a lone pair of the oxygen [7].

Table 1 MP2 optimum X…O separations (Å) and X…O=C angles (degrees), MP2 interaction energies ΔE (kcal mol^{-1}), estimated dispersion energies ΔE_{corr} (kcal mol^{-1}) and B3PW91/6-311G* σ-hole electrostatic potential maxima $V_{S,max}$ (kcal mol^{-1}) of halogens X

	MP2 (X…O)	MP2 (X…O=C)	ΔE (MP2)	ΔE_{corr}	$V_{S,max}$
Complex					
Cl-benz	3.16	118	−1.30	−1.98	5.3
Cl-benz-2F	3.10	120	−1.74	−1.85	11.9
Cl-benz-5F	3.00	121	−2.63	−2.00	18.9
Br-benz	3.13	122	−2.23	−2.44	12.2
Br-benz-2F	3.04	123	−2.78	−2.17	18.4
Br-benz-5F	2.91	124	−4.09	−2.36	27.2

As has been found in earlier studies [7, 8, 19], there is a good correlation between the interaction energies and the $V_{S,max}$; R^2=0.955. As the σ-hole becomes more positive, the halogen bond becomes stronger (ΔE more negative).

DFT-SAPT results

Table 2 contains the DFT-SAPT optimum X…O separations, the interaction energies ΔE and the estimated electrostatic and dispersion contributions to the ΔE, E_{electr} and E_{disp}. The MP2 and DFT-SAPT X…O distances and ΔE are very similar but do show a certain pattern: The MP2 X…O are shorter and the ΔE more negative, but only by an average of 0.02 Å and 0.11 kcal mol^{-1}. It will be noted that, for all six complexes, our DFT-SAPT calculations indicate that the largest attractive contributions come from the dispersion and electrostatic terms; induction effects play a smaller role in these complexes (see Figs. S1–S6 in supplementary material).

The E_{electr} represent largely the electrostatic interactions between the unperturbed ground states of the halobenzenes and acetone. E_{electr} is more negative in direct proportion to the σ-hole $V_{S,max}$ of the halobenzene becoming more positive; R^2=0.951. Both the MP2 and the DFT-SAPT interaction energies ΔE correlate remarkably well with the DFT-SAPT E_{electr}; the linear R^2 are 0.9997 and 0.997, respectively.

The E_{disp} in Table 2, which are the DFT-SAPT predictions of the dispersion components of the interactions, are to be compared to the ΔE_{corr} in Table 1, which were obtained by applying Eq. (2). The two sets of values are within 1.5 kcal mol^{-1} of each other, with the DFT-SAPT always being the more negative, but the trends are different. E_{disp} becomes monotonically more negative in going from Cl-benz to Br-benz-5F, while ΔE_{corr} tends to hover within one small range for the chlorine systems and another for the bromine. However both E_{disp} and ΔE_{corr} indicate that the dispersion contributions to the interactions are greater for the bromine derivatives. This is consistent with the higher polarizability of the bromine atom, since dispersion is a function of polarizability [21, 23, 28, 29].

Table 2 Selected DFT-SAPT results: Optimum X…O separations (Å), electrostatic and dispersion energies E_{electr} and E_{disp} (kcal mol^{-1}), and total interaction energies ΔE (kcal mol^{-1}). The X…O=C angles are the same as in Table 1

	DFT-SAPT (X…O)	DFT-SAPT E_{electr}	DFT-SAPT E_{disp}	DFT-SAPT ΔE
Complex				
Cl-benz	3.19	−1.08	−2.32	−1.19
Cl-benz-2F	3.13	−1.79	−2.49	−1.71
Cl-benz-5F	3.00	−3.19	−2.99	−2.61
Br-benz	3.15	−2.57	−3.11	−2.09
Br-benz-2F	3.05	−3.53	−3.20	−2.64
Br-benz-5F	2.93	−5.66	−3.80	−3.90

Energy curves

Figures 4, 5, 6, 7, 8 and 9 show, for each complex, the variation with X…O separation of ΔE(MP2), ΔE_{corr}, E_{disp} and E_{electr}. Only ΔE(MP2) passes through a minimum; the others represent attractive components of the interactions and decrease monotonically.

For each complex, the two measures of the dispersion energy, ΔE_{corr} and E_{disp}, are nearly identical at large X…O separations but begin to move apart as the equilibrium X…O distance is approached. E_{disp} is always more negative. For the three chlorobenzenes, the E_{disp} curves are almost superimposable (Fig. 10), and the ΔE_{corr} are also very similar (Fig. 11). The bromobenzene curves are somewhat more negative (Figs. 10 and 11) as would be expected from the greater polarizability of bromine. There is an interesting tendency for E_{disp} and especially ΔE_{corr} to become less negative as the number of fluorines increases. This is particularly marked in comparing Br-benz to Br-benz-2F and Br-benz-5F.

Proceeding to E_{electr} and looking first at the chlorine systems, at large X…O separations the E_{electr} curves are less negative than ΔE_{corr} and E_{disp} but then they begin to descend rapidly (Figs. 4, 5, and 6), more so as the σ-hole $V_{S,max}$ is more positive, and eventually they cross both ΔE_{corr} and E_{disp}. The more positive $V_{S,max}$, the larger the X…O at which the crossing occurs. Tables 1 and 2 show that as the

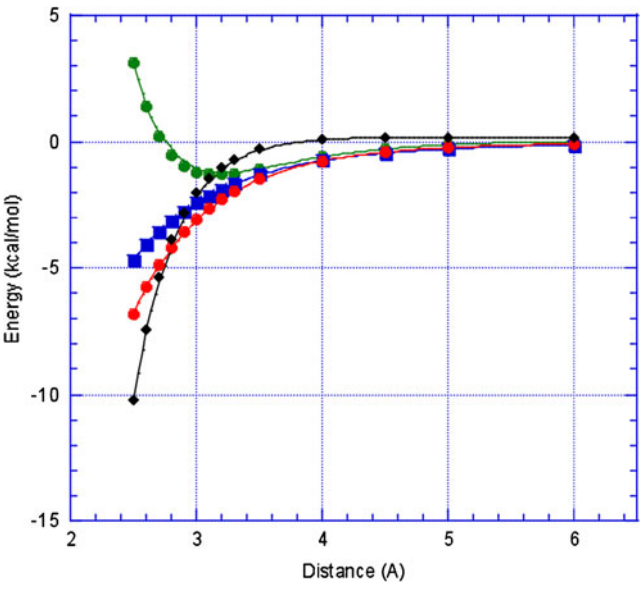

Fig. 4 Computed energy quantities for Cl-benz, as function of Cl…O separation. Green circles denote ΔE(MP2), blue squares denote ΔE_{corr}=ΔE(MP2) - ΔE(HF), red circles denote DFT-SAPT E_{disp} and black diamonds denote DFT-SAPT E_{electr}

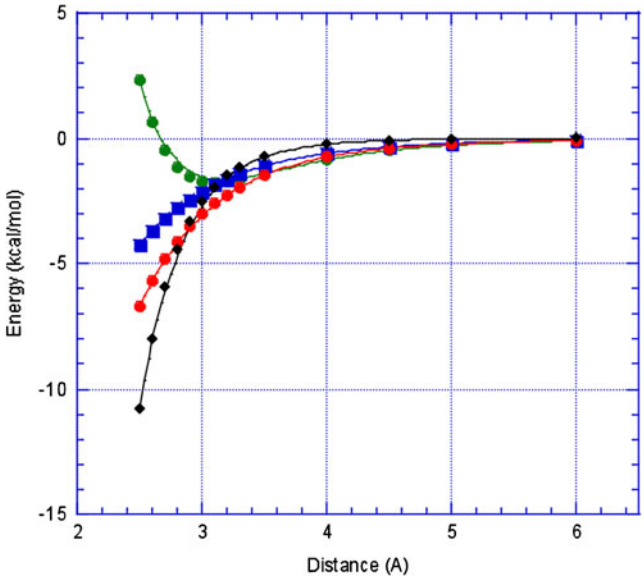

Fig. 5 Computed energy quantities for Cl-benz-2F, as function of Cl…O separation. Green circles denote ΔE(MP2), blue squares denote ΔE_{corr}=ΔE(MP2) - ΔE(HF), red circles denote DFT-SAPT E_{disp} and black diamonds denote DFT-SAPT E_{electr}

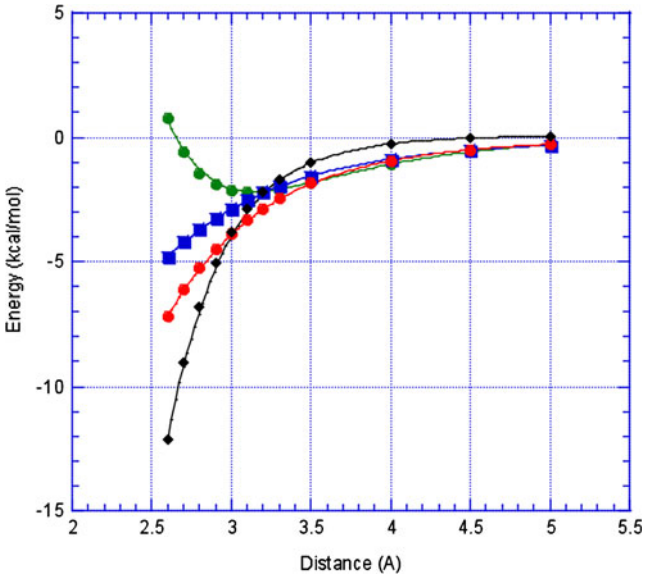

Fig. 7 Computed energy quantities for Br-benz, as function of Br…O separation. Green circles denote ΔE(MP2), blue squares denote ΔE_{corr}=ΔE(MP2) - ΔE(HF), red circles denote DFT-SAPT E_{disp} and black diamonds denote DFT-SAPT E_{electr}

number of fluorines increases and the chlorine σ-hole $V_{S,max}$ becomes more positive, the magnitude of E_{electr} at the equilibrium X…O distance approaches and finally, for Cl-benz-5F, exceeds both ΔE_{corr} and E_{disp}.

For the three bromine systems, the E_{electr} curves are more negative than for the chlorine (Figs. 4, 5, 6, 7, 8 and 9 and Fig. 12). They begin their rapid descents at larger X…O, so that at the equilibrium separations E_{electr} is more negative than both ΔE_{corr} and E_{disp} already for Br-benz-2F. For Br-benz-5F, E_{electr} is below ΔE_{corr} and E_{disp} even at large X…O. These trends are again associated with the bromine σ-hole $V_{S,max}$ being increasingly positive.

Discussion and summary

A general pattern is evident in Figs. 4, 5, 6, 7, 8, 9, 10, 11 and 12. As the halobenzene and acetone initially approach

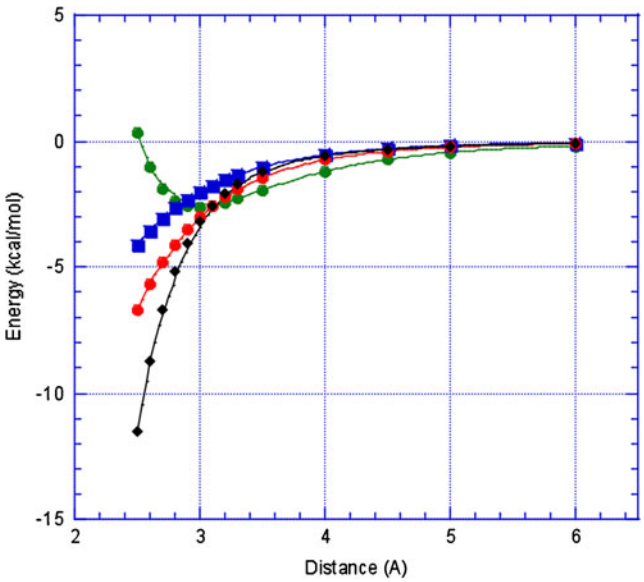

Fig. 6 Energy quantities for Cl-benz-5F, as function of Cl…O separation. Green circles denote ΔE(MP2), blue squares denote ΔE_{corr}=ΔE(MP2) - ΔE(HF), red circles denote DFT-SAPT E_{disp} and black diamonds denote DFT-SAPT E_{electr}

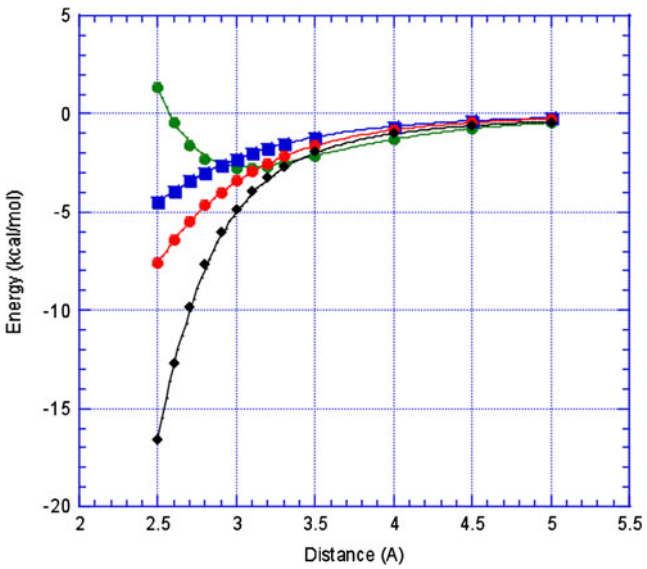

Fig. 8 Computed energy quantities for Br-benz-2F, as function of Br…O separation. Green circles denote ΔE(MP2), blue squares denote ΔE_{corr}=ΔE(MP2) - ΔE(HF), red circles denote DFT-SAPT E_{disp} and black diamonds denote DFT-SAPT E_{electr}

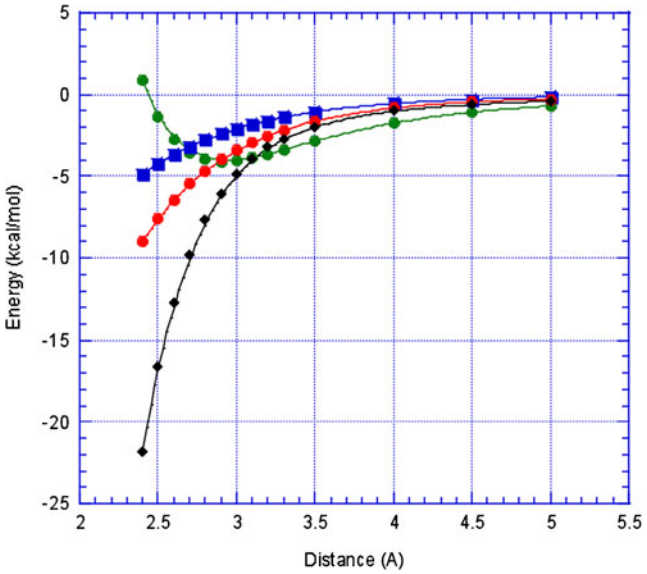

Fig. 9 Computed energy quantities for Br-benz-5F, as function of Br…O separation. Green circles denote ΔE(MP2), blue squares denote ΔE_{corr}=ΔE(MP2) - ΔE(HF), red circles denote DFT-SAPT E_{disp} and black diamonds denote DFT-SAPT E_{electr}

each other, at large separations, both the electrostatic and the dispersion components of the interaction energies become more negative (stronger) in a gradual manner. For dispersion, this continues at shorter X…O distances. However the electrostatic component, at an X…O of roughly 3.5 Å, begins to decrease rapidly. The relative contributions of dispersion and electrostatics at the equilibrium separations depend upon the rates of change of the respective curves, which now may differ considerably, depending on the size and charge of the halogen σ-hole. Accordingly, as is seen in Tables 1 and 2, dispersion dominates at equilibrium in some complexes and electrostatics in others. However they are

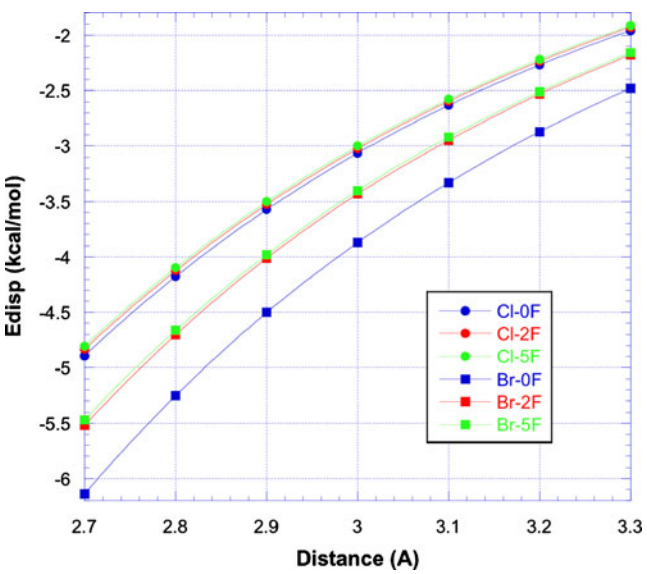

Fig. 10 Computed DFT-SAPT E_{disp} as function of X…O separation

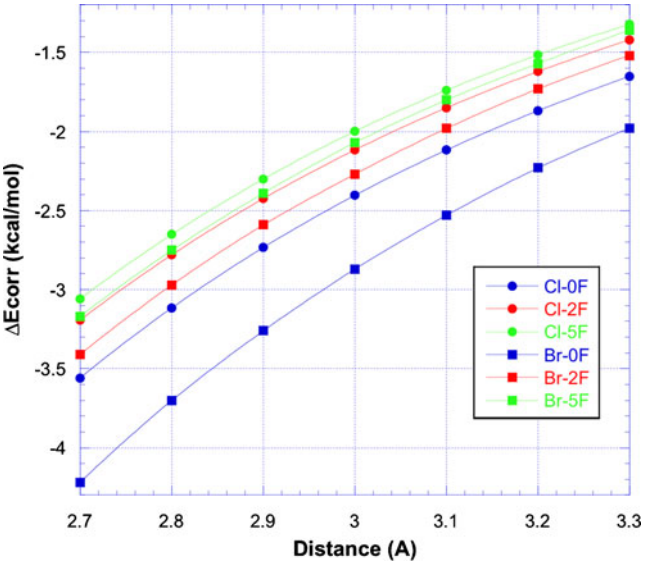

Fig. 11 Computed ΔE_{corr} as function of X…O separation

usually of comparable magnitudes (unless the σ-hole $V_{S,max}$ is very positive) and this is likely to be the case even when polarization is taken into account, since it can be expected to normally be less than about 25% of the magnitude of E_{electr} [7, 26, 27].

Figure 12 shows that for the three chlorobenzenes, as for the three bromobenzenes, the electrostatic interaction is strengthened (E_{electr} is more negative) as the σ-hole $V_{S,max}$ increases. This is entirely as expected. What is more interesting is that the dispersion interaction weakens in the same direction (Figs. 10 and 11, E_{disp}. and especially ΔE_{corr} becoming less negative). This can be explained by noting that the shifting of valence electronic charge that gives rise to a positive σ-hole potential also diminishes the local

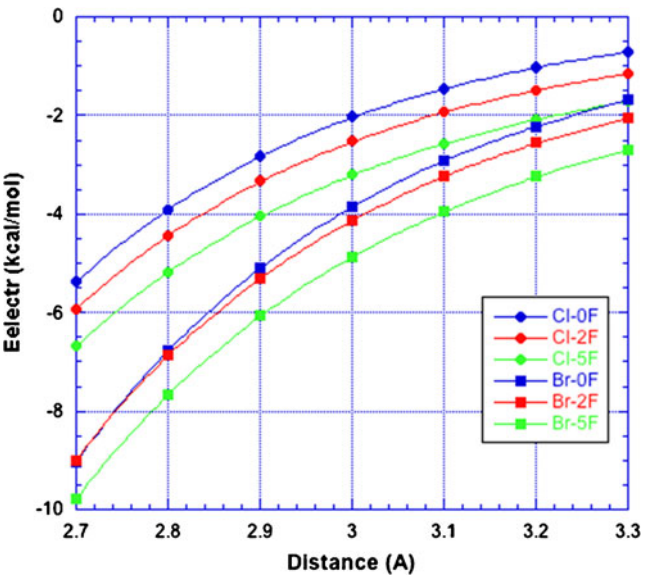

Fig. 12 Computed DFT-SAPT E_{electr} as function of X…O separation

polarizability of the halogen. An effective measure of local polarizability has been demonstrated to be the local surface ionization energy $I_S(\mathbf{r})$ [52, 53] (they vary inversely). For the free chlorine atom, the computed value is 11.03 eV [B3PW91/6-311G(d)], compared to 13.32 eV for Cl-benz, 13.87 eV for Cl-benz-2F and 14.70 eV for Cl-benz-5F. The corresponding magnitudes for the free bromine atom and the three bromobenzenes are 9.98 eV, 12.43 eV, 12.97 eV and 13. 83 eV. Thus the increases in $V_{S,max}$ are accompanied by significant decreases in polarizability in the vicinities of the σ-holes and a consequent diminishing of dispersion energies. It follows that the dominant role that has been found for E_{electr} when $V_{S,max}$ is very positive [7, 20] reflects not only a strengthened electrostatic interaction but also weakened dispersion.

Finally we wish to comment on the fact that the sequence of the six E_{electr} curves in Fig. 12 does not reflect the fact that the σ-hole $V_{S,max}$ of Cl-benz-2F and Br-benz are essentially the same, as are those of Cl-benz-5F and Br-benz-2F. This is presumably because E_{electr} represents the electrostatic interaction of acetone with the entire halobenzene molecule not just its chlorine or bromine σ-hole. The E_{electr} and ΔE *at equilibrium* do correlate with $V_{S,max}$, as already pointed out; however the equilibrium points are at different X…O distances for the various complexes.

Acknowledgments This work was a part of research Project No. Z40550506 of the Institute of Organic Chemistry and Biochemistry, ASCR and was supported by the Operational Program Research and Development for Innovations - European Regional Development Fund (Project CZ.1.05/2.1.00/03.0058 of the MEYS of the CR). The support of Praemium Academiae, ASCR, awarded to P.H. in 2007 is acknowledged. This work was also supported by the Czech Science Foundation (P208/12/G016).

References

1. Metrangolo P, Neukirch H, Pilati T, Resnati G (2005) Acc Chem Res 38:386–395
2. Metrangolo P, Resnati G (2008) Halogen bonding: fundamentals and applications. Springer, Berlin
3. Auffinger P, Hays FA, Westhof E, Ho PS (2004) Proc Nat Acad Sci USA 101:16789–16794
4. Murray JS, Riley KE, Politzer P, Clark T (2010) Aust J Chem 63:1598–1607
5. Riley KE, Hobza P (2011) Cryst Growth Des 11:4272–4278. doi:10.1021/Cg200882f
6. Hardegger LA, Kuhn B, Spinnler B, Anselm L, Ecabert R, Stihle M, Gsell B, Thoma R, Diez J, Benz J, Plancher JM, Hartmann G, Banner DW, Haap W, Diederich F (2011) Angew Chem Int Ed 50:314–318. doi:10.1002/Anie.201006781
7. Riley KE, Murray JS, Concha MC, Politzer P, Hobza P (2009) J Chem Theor Comput 5:155–163
8. Riley KE, Murray JS, Fanfrlik J, Rezac J, Sola RJ, Concha MC, Ramos FM, Politzer P (2011) J Mol Model 17:3309–3318
9. Politzer P, Murray JS (2009) In: Leszczynski J, Shukla M (eds) Practical Aspects of Computational Chemistry. Springer, Heidelberg, pp 149–163
10. Politzer P, Murray JS, Clark T (2010) Phys Chem Chem Phys 12:7748–7757
11. Metrangolo P, Murray JS, Pilati T, Politzer P, Resnati G, Terraneo G (2011) Crystal Growth Design 11:4238–4246. doi:10.1021/Cg200888n
12. Ikuta S (1990) J Mol Struct (THEOCHEM) 205:191–201
13. Nyburg SC, Wong-Ng W (1979) Proc Royal Soc London A 367:29–45
14. Price SL, Stone AJ, Lucas J, Rowland RS, Thornley AE (1994) J Am Chem Soc 116:4910–4918
15. Stevens ED (1979) Mol Phys 37:27–45
16. Tsirelson VG, Zou PF, Tang TH, Bader RFW (1995) Acta Cryst A51:143–153
17. Clark T, Hennemann M, Murray JS, Politzer P (2007) J Mol Model 13:291–296
18. Hennemann M, Murray JS, Politzer P, Riley KE, Clark T (2012) J Mol Model doi: 10.1007/s00894-011-1263-5
19. Shields Z, Murray JS, Politzer P (2010) Int J Quantum Chem 110:2823–2832
20. Riley KE, Hobza P (2008) J Chem Theor Comput 4:232–242. doi:10.1021/Ct700216w
21. Chalasinski G, Szczesniak MM (2000) Chem Rev 100:4227–4252. doi:10.1021/Cr990048z
22. Hobza P, Zahradnik R, Muller-Dethlefs K (2006) Coll Czech Chem Commun 71:443–531
23. Jeziorski B, Moszynski R, Szalewicz K (1994) Chem Rev 94:1887–1930
24. Chen J, Martinez TJ (2007) Chem Phys Lett 438:315–320
25. Sokalski WA, Roszak SM (1991) J Mol Struct (THEOCHEM) 80:387–400
26. Ma YG, Politzer P (2004) J Chem Phys 120:3152–3157. doi:10.1063/1.1640991
27. Kitaura K, Morokuma K (1976) Int J Quantum Chem 10:325–340
28. Cramer CJ (2002) Essentials of computational chemistry. Wiley, Chichester
29. Hobza P, Zahradnik R (1992) Int J Quantum Chem 42:581–590
30. Jaffe RL, Smith GD (1996) J Chem Phys 105:2780–2788
31. Shishkin OV (2008) Chem Phys Lett 458:96–100. doi:10.1016/J.Cplett.2008.04.106
32. Shishkin OV, Zubatyuk RI, Dyakonenko VV, Lepetit C, Chauvin R (2011) Phys Chem Chem Phys 13:6837–6848. doi:10.1039/C0cp02666b
33. Boys SF, Bernardi F (1970) Mol Phys 19:553–566
34. Hesselmann A, Jansen G (2003) Phys Chem Chem Phys 5:5010–5014. doi:10.1039/B310529f
35. Hesselmann A, Jansen G, Schutz M (2005) J Chem Phys 122:014103
36. Perdew JP, Burke K, Ernzerhof M (1996) Phys Rev Lett 77:3865
37. Dunning TH (1989) J Chem Phys 90:1007–1023
38. Tekin A, Jansen G (2007) Phys Chem Chem Phys 9:1680–1687
39. Politzer P, Truhlar DG (1981) Chemical applications of atomic and molecular electrostatic potentials. Plenum, New York
40. Stewart RF (1979) Chem Phys Lett 65:335–342
41. Politzer P, Murray JS (2002) Theor Chem Acc 108:134–142
42. Ayers PW (2007) Chem Phys Lett 438:148–152. doi:10.1016/J.Cplett.2007.02.070
43. Politzer P (2004) Theor Chem Acc 111:395–399. doi:10.1007/S00214-003-0533-4
44. Murray JS, Politzer P (2011) WIREs Comput Mol Sci 1:153–163. doi:10.1002/Wcms.19
45. Bulat FA, Toro-Labbé A, Brinck T, Murray JS, Politzer P (2010) J Mol Model 16:1679–1691

46. Bader RFW, Carroll MT, Cheeseman JR, Chang C (1987) J Am Chem Soc 109:7968–7979
47. Murray-Rust P, Motherwell WDS (1979) J Am Chem Soc 101:4374–4376
48. Murray-Rust P, Stallings WC, Monti CT, Preston RK, Glusker JP (1983) J Am Chem Soc 105:3206–3214
49. Politzer P, Murray JS, Concha MC (2008) J Mol Model 14:659–665. doi:10.1007/S00894-008-0280-5
50. Wang FF, Hou JH, Li ZR, Wu D, Li Y, Lu ZY, Cao WL (2007) J Chem Phys 126:144301. doi:Artn144301Doi10.1063/1.2715559
51. Bondi A (1964) J Phys Chem 68:441–451
52. Jin P, Murray JS, Politzer P (2004) Int J Quantum Chem 96:394–401. doi:10.1002/Qua.10717
53. Politzer P, Murray JS, Bulat FA (2010) J Mol Model 16:1731–1742. doi:10.1007/S00894-010-0709-5